Lasers in Medical Science (2019) 34:1829–1839
https://doi.org/10.1007/s10103-019-02778-5

ORIGINAL ARTICLE

A transient protective effect of low-level laser irradiation against disuse-induced atrophy of rats

Yung-Ting Kou[1,2] · Hui-Tien Liu[3] · Chun-Yin Hou[4] · Chuang-Yu Lin[5] · Chung-Min Tsai[3] · Hsi Chang[2,6]

Received: 30 November 2018 / Accepted: 18 March 2019 / Published online: 4 April 2019

Abstract

Satellite cells, a population of skeletal muscular stem cells, are generally recognized as the main and, possibly, the sole source of postnatal muscle regeneration. Previous studies have revealed the potential of low-level laser (LLL) irradiation in promoting satellite cell proliferation, which, thereby, boosts the recovery of skeletal muscle from atrophy. The purpose of this study is to investigate the beneficial effect of LLL on disuse-induced atrophy. The optimal irradiation condition of LLL (808 nm) enhancing the proliferation of $Pax7^{+ve}$ cells, isolated from tibialis anterior (TA) muscle, was examined and applied on TA muscle of disuse-induced atrophy model of the rats accordingly. Healthy rats were used as the control. On one hand, transiently, LLL was able to postpone the progression of atrophy for 1 week through a reduction of apoptosis in $Pax7^{-ve}MyoD^{+ve}$ (myocyte) population. Simultaneously, a significant enhancement was observed in $Pax7^{+ve}MyoD^{+ve}$ population; however, most of the increased cells underwent apoptosis since the second week, which suggested an impaired maturation of the population. On the other hand, in normal control rats with LLL irradiation, a significant increase in $Pax7^{+ve}MyoD^{+ve}$ cells and a significant decrease of apoptosis were observed. As a result, a strengthened muscle contraction was observed. Our data showed the capability of LLL in postponing the progression of disuse-induced atrophy for the first time. Furthermore, the result of normal rats with LLL irradiation showed the effectiveness of LLL to strengthen muscle contraction in healthy control.

Keywords Low-level laser irradiation · Disuse-induced atrophy · Myoblast · Enhanced proliferation · Apoptosis · Transient protective effect

Introduction

Skeletal muscle is the main constituent of the musculoskeletal system, one of the largest organ systems of the body, accounting for 40–50% of the total body weight [1, 2]. Skeletal muscles are broadly distributed thereby to confer the motor function to individuals. In fact, the impairment of the skeletal muscle system not only affects motor function but also influences the emotional behavior, mental health, and quality of life of individuals [3]. In some severe cases, a life-threatening complication, such as respiratory failure, can also occur [4]. Although the skeletal muscle is a highly differentiated tissue containing multinucleate myofibers, it still exhibits a capacity for morphological and functional adaption. The integrity of the skeletal muscle relies on a small population of skeletal muscle stem cell, called the satellite cell (SC), which is located underneath the basal lamina [5]. Satellite cells are normally kept under a quiescent state and are activated in response to the needs for myonuclear turnover and myofiber hypertrophy through the proliferation and differentiation of SCs. Both the

Yung-Ting Kou and Hui-Tien Liu contribute equally.

Electronic supplementary material The online version of this article (https://doi.org/10.1007/s10103-019-02778-5) contains supplementary material, which is available to authorized users.

✉ Hsi Chang
jamesc@h.tmu.edu.tw

1 Department of Pediatrics, Shung Ho Hospital, Taipei Medical University, Taipei, Taiwan

2 Department of Pediatrics, School of Medicine, College of Medicine, Taipei Medical University, Taipei, Taiwan

3 Graduate Institute of Medical Sciences, College of Medicine, Taipei Medical University, Taipei, Taiwan

4 Department of Family Medicine, Taipei City Hospital, Taipei, Taiwan

5 Department of Clinical Application, Center for iPS Cell Research and Application (CiRA), Kyoto University, Kyoto, Japan

6 Department of Pediatrics, Taipei Medical University Hospital, Taipei, Taiwan

maintenance of quiescence and the activation of the SC involve complex processes with various transcription factors, among which Pax7 and MyoD show particular importance. Pax7 is a well-known satellite cell marker [6], whereas MyoD is a marker of myogenic lineage commitment [7]. A quiescent-state SC is known to express Pax7 but not MyoD ($Pax7^{+ve}MyoD^{-ve}$) for its cell marker [8, 9]. However, MyoD expression is known to be up-regulated when SC is under an activated state ($Pax7^{+ve}MyoD^{+ve}$), and these $Pax7^{+ve}MyoD^{+ve}$ SCs are also called as "myoblasts" alternatively. Responding the signal of regeneration, the activated SCs first proliferate to increase cell count and later differentiate and committed into the myogenic lineage by maintaining MyoD while down-regulating Pax7 expression ($Pax7^{-ve}MyoD^{+ve}$) [10, 11]. Since SCs are known to be the main and, possibly, the sole source of postnatal muscle regeneration [12], some activated SCs return to the quiescent state by maintaining Pax7 but down-regulating MyoD expression to prepare for future use, thus preventing the depletion of the SC reservoir [8]. As the supply–demand of myogenic cells maintains balanced, it ensures that the total skeletal muscle mass remains within the so-called healthy level. Conversely, in the event of homeostasis disruption and supply–demand imbalance, skeletal atrophy (the loss of muscle mass) occurs [13, 14]. Muscular atrophy can be caused by various reasons [15–19], and disuse may be one of the frequent reasons to be encountered clinically. In addition, according to the previous reports, the pathological formation of disuse-induced atrophies is suspected to be closely related to the reduction of satellite cells through the mechanism of apoptosis [20, 21].

On the other hand, low-level laser (LLL) irradiation has been shown to modulate various biological processes; for example, it can increase mitochondrial respiration, thus enhancing ATP production [22]. Moreover, LLL irradiation exerts positive effects on wound healing by prohibiting tissue fibrosis [23] and promoting angiogenesis [24]. These positive effects have been observed on the skin [25], bone [26], nervous system [27], and skeletal muscle [28–31]. Ben-Dov et al. [32] determined the effect of LLL on primary-cultured rat myogenic cells; the results clearly demonstrated the in vitro effect of LLL on inducing cell cycle regulatory protein expression, thus increasing cell proliferation and inhibiting cell differentiation and fusion [32, 33]. Furthermore, Shefer et al. [34] reported the protective role of LLL against in vitro apoptosis of SCs, and a recent study reported the effectiveness of LLL in boosting recovery in a disuse-related atrophy rat model [31, 35]. Considering all these results, we conjecture that LLL may be able to exert a protective effect on skeletal muscle and delay the progression of disuse-induced atrophy.

The objective of this study is to evaluate the protective effect of LLL on disuse-induced atrophy model. We applied LLL irradiation on the tibialis anterior (TA) muscle of rat of disuse-induced atrophy model and evaluated its effect by subjecting the muscle to morphological, histological, electrophysiological, and motor functional analyses. As mentioned previously, disuse-induced muscular atrophy is suspected to be involved with SC reduction through its apoptosis. Therefore, the temporal sequential changes in the cell count of apoptotic SC in activated ($Pax7^{+ve}MyoD^{+ve}Tunel^{+ve}$) and myogenic lineage-committed ($Pax7^{-ve}MyoD^{+ve}Tunel^{+ve}$) cells were assessed through the combination of immunostaining and terminal deoxynucleotidyl transferase dUTP nick-end labeling (TUNEL) assay.

Material and methods

Animals

Male Sprague–Dawley rats were used for the current study. All animal handling procedures were performed in accordance with the Guide for the Care and Use of Laboratory Animals, published by the National Institutes of Health (NIH Publication No. 85-23, revised 1996), and the Guidelines of the Animal Research Committee of Taipei Medical University. The experimental rats were divided randomly into the following four groups: control (Con), control with LLL (Con-La), disuse (Dis), and disuse with LLL (Dis-La).

Low-level laser irradiation

The detailed irradiation was performed as follows: A Ga-Al-As laser machine (custom-made model, Transverse Industries Company, Taipei, Taiwan) with a wavelength of 808 nm, continuous mode, and power density or irradiance of 27.79 mW/cm^2 was used for the whole experiment. The laser machine was composed of 12 laser lenses with arrangement of 6 × 2 array (length 10.8 cm × width 3.5 cm). The output power of each laser lens was 110 mW, and a total of 12 laser lenses sum up with total output power of 1320 mW. The output area at the end of each lens hood was 0.0824 cm^2, and the total output area was 0.9888 cm^2. The illuminated area on 24-well plate after divergence of laser beams under vertical distance (10.8 cm) between the front of the lens hoods and the base of the plate was 3.8 cm × 12.5 cm = 47.5 cm^2, which yielded the power density or irradiance of 27.79 mW/cm^2. The energy density of the irradiation duration at 3, 7, 10, and 15 s was 83.37, 195.30, 277.90, and 416.85 mJ/cm^2, respectively. The maintenance, which includes calibration, has been performed every 6 months to keep the machine in best condition. For the cultivated cells, after myogenic progenitor cells (MPCs) were isolated from TA muscle and seeded onto 24-well plate, LLL irradiation was applied onto the culture-well plates inside the laminar flow bench directly. Each well was irradiated for 3 s (0.07 J/day), 7 s (0.2 J/day), 10 s (0.29 J/day), and 15 s (4.3 J/day), respectively. To further correlate in vitro experiments to

in vivo, we next performed LLL experiments on disuse models. The LLL irradiations of 7 s (18.66 J/rat/day) were performed immediately after the damage (disuse) and once daily for 7, 14, and 21 days consecutively before evaluation. The hair of the right leg was shaved before irradiation to ensure that the lens hoods could properly attach to the circle-marked spot above the TA muscle and that a better penetration was guaranteed. In brief, two adjacent laser lenses, with 1.8 cm in length, between two centers of laser beams were exposed while the rest of the 10 laser lenses were blocked by aluminum sheet. The vertical length of each lens hood was 1.1 cm, and the laser beam with 2 mm in diameter diverged into an eclipse with major axis and minor axis at 3.5 and 3.0 mm, respectively, at the front of the lens hood. Hence, the irradiance area of each laser beam was 0.0825 cm^2, and the power density of each beam was 1.33 W/cm^2 accordingly. Next, the right leg, with two superficial circled marks on the skin upon TA muscle, was attached to two adjacent lens hoods with inner diameter of 1.2 cm each. Then, the LLL irradiation for 7 s was performed. Collectively, the energy density of two laser beams on the surface of the TA muscle was 18.66 J/cm^2 per rat. Furthermore, rats in the control and disuse groups receive sham procedure, in which the right legs were attached to lens hoods for 7 s with power supply turned off.

Isolation and differentiation of myogenic progenitor cell

TA muscles of the healthy rats were isolated and cut or minced into small pieces by scissor sterilely. Then, the minced TA muscle was incubated in DMEM containing 0.5% type I collagenase (Worthington, USA) at 37 °C for 90 min. The isolated interstitial and myofiber-associated cells were passed through 40 μm cell strainer (Falcon, USA) and centrifuged at 1200 rpm for 3 min. The isolated cells were transferred to 0.1% gelatin-coated 24-well culture plate (Falcon) in density of 1×10^5/well with differentiation medium which consisted of DMEM supplemented with penicillin/streptomycin, 0.1 mM non-essential amino acids, 0.1 mM 2-mercaptonethanol, 5% horse serum (HS), and 10% fetal bovine serum (FBS). Pax7 immunostaining together with bromodeoxyuridine (BrdU) proliferation assay or MTT (3-(4,5-dimethylthiazol-2-yl)-2,5-diphenyltetrazolium bromide) assay was performed 48 h after cell plating.

Disuse model

Male Sprague–Dawley rats (190–210 g) were maintained in an animal room under standard housing conditions. One to three rats were kept per cage (9 in. × 12 in. × 9 in.). All animals were kept in a quiet animal facility with temperature of 21 to 23 °C and a relative humidity of 30 to 70% under a 12-h light/dark cycle. The rats were equipped with a modified version of hand-made restriction suit that was originally designed by Benedini-Elias et al. [13] to inhibit the activity of their Rt. lower limbs during the whole experimental period (Suppl. Fig. 1). All animals were confirmed to be accessible to food and water. In addition, all the restricted rats were supervised daily to ensure no erosion nor wound formed at the restricted limbs.

Immunocytochemical analysis (include BrdU and TUNEL assays)

Immunocytochemical analysis was performed as described previously [36]. Briefly, the cultured cells were fixed in 2% paraformaldehyde (PFA). Mouse anti-Pax7 (MAB1675, R&D Systems, Minneapolis, MN, USA; 1:50) and rabbit anti-MyoD (bs-2442R, Bioss Antibodies Inc., Massachusetts, USA; 1:50) were used for Pax7 and MyoD staining, respectively. Rabbit polyclonal anti-BrdU antibody (ab152095; Abcam, Cambridge, UK) and the fluorescein in situ cell death detection kit, terminal deoxynucleotidyl transferase dUTP nick-end labeling (TUNEL; 11 684 795 910; Roche, Mannheim, Germany), were used following product guidance. As for the secondary antibodies, the Cy5-conjugated AffiniPure Donkey anti-mouse IgG (715-175-151, Jackson ImmunoResearch Laboratory, West Grove, PA, USA) and Cy3-conjugated AffiniPure Donkey anti-rabbit IgG (711-165-152, Jackson ImmunoResearch Laboratory, West Grove, PA, USA) were used. Hoechst 33324 (H3570; Invitrogen, Paisley, UK) was used for nuclear staining. The samples were analyzed through fluorescence microscopy (Olympus, Tokyo, Japan) or an AS-MDW system (Leica Microsystems, Wetzlar, Germany). Micrographs were obtained using AxioCam (Carl Zeiss Vision, Hallbergmoos, Germany) or the AS-MDW system (Leica Microsystems). The cell counting was performed 48 h after plating. For cell counting analysis, Pax7 single-positive ($Pax7^{+ve}$) and Pax7-BrdU double-positive ($Pax7^{+ve} + BrdU^{+ve}$) cells were enumerated per field (× 100), respectively, in the culture dish. The average and standard deviation were calculated from 10 fields for each culture dish sample. The ratio of proliferating SC within each irradiated group was acquired by the following formulation: ($Pax7^{+ve}BrdU^{+ve}$) / $Pax7^{+ve}$ / control. In the muscle sections, Pax7-MyoD double-positive ($Pax7^{+ve}MyoD^{+ve}$) and apoptotic Pax7-MyoD double-positive ($Pax7^{+ve}MyoD^{+ve}TUNEL^{+ve}$) cells were enumerated per field (× 100). As for the calculation in culture dishes, the average and standard deviation were calculated from 10 fields for each TA muscle sample per rat. Later, the average and standard deviation of the group were calculated by collecting the data of all rats in each group.

MTT assay

As with the BrdU assay, the MTT assay was performed 48 h after seeding of the MPCs. The detailed procedure of the MTT assay is as follows: MPCs were incubated with 450 μM MTT (Sigma-Aldrich, St. Louis, MO) for 3 h, and, then, centrifuged at 1800 rpm for 10 min at room temperature to remove the supernatant. Afterwards, formazan was extracted from pelleted cells with 600 μl of DMSO for 15 min. The amount of MTT-formazan was determined by 570 nm absorbance with 655 nm as the wavelength reference.

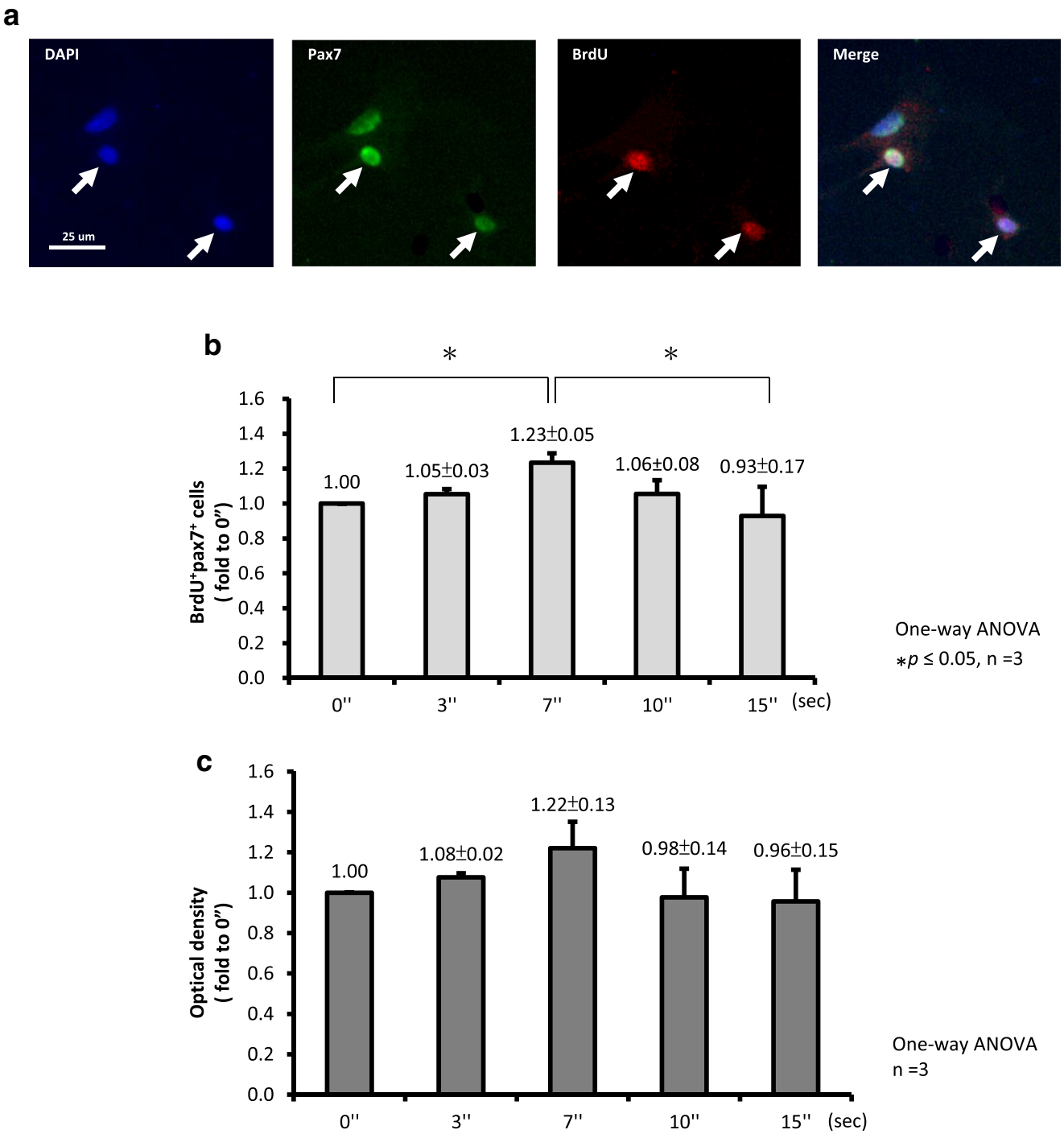

Fig. 1 LLL irradiation for 7 s effectively increases the proliferation of Pax7^{+ve} cells isolated from TA muscle. **a** Proliferating Pax7^{+ve} satellite cells (Pax7^{+ve} BrdU^{+ve}) derived from primary-cultured TA muscle (white arrow) were enumerated. Bar, 25 μm. **b** The 7 s irradiation condition demonstrated the most favorable proliferation rate of satellite cells (1.23 ± 0.05, $p \leq 0.05$). **c** Consistent with the result of the BrdU assay, the MTT assay demonstrated 7 s irradiation as the optimal condition for cell metabolic activity (1.22 ± 0.13, $p = 0.08$)

Hematoxylin and eosin staining

TA muscles were isolated and frozen in liquid nitrogen-cooled isopentane. Serial transverse 5-μm-thick cryosections of the muscle were cut and transferred onto slides. Later, the slides were incubated with Mayer's hematoxylin solution for 1 min and washed with running water for 5 min. After incubation in an eosin solution containing one drop of acetic acid, the sections were rinsed quickly in water, hydrated using a gradient of ethanol solutions at 70, 80, 90, 95, and 100%, mounted with xylene-based mounting media, and covered with cover glass.

Electromyogram

The TA muscle was examined. The rats that underwent electromyogram (EMG) were anesthetized with pentobarbital sodium (intraperitoneally, 30 mg/kg body weight) during the

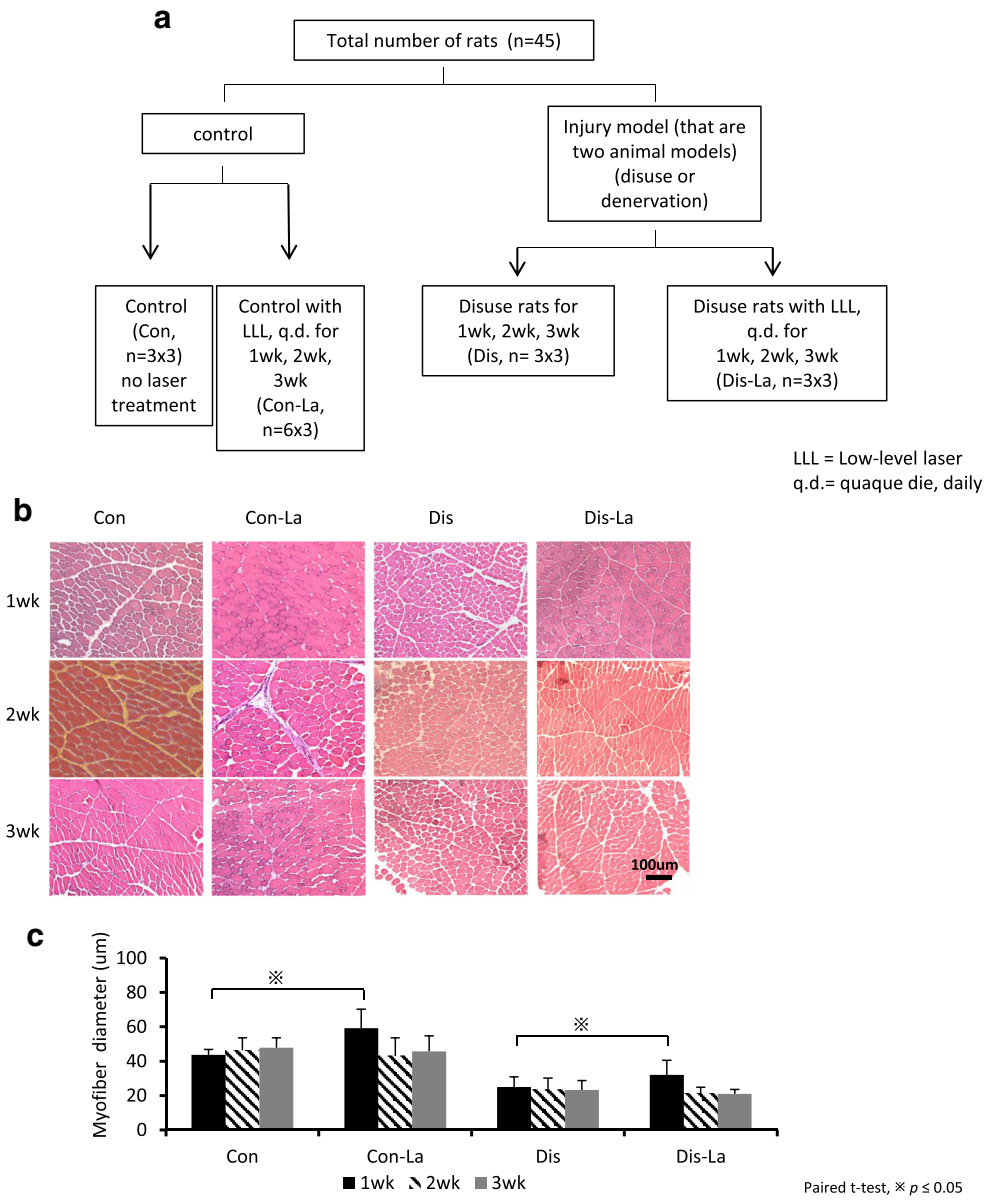

		Con	Con-La	Dis	Dis-La
1wk	Ave	43.7	59.2	24.95	32.05
	SD	3.19	11.04	5.86	8.42
2wk	Ave	46.2	39.7	27.4	21.27
	SD	7.4	10.2	9.81	3.6
3wk	Ave	47.9	45.7	23.25	21.03
	SD	5.64	9.1	5.45	2.54

(um)

Fig. 2 LLL irradiation temporarily delays atrophy progression by preserving the muscle mass in the disuse-induced atrophy model. **a** Experimental rats were divided into the following four groups to evaluate the effect of LLL against disuse-induced atrophy: control (Con, $n = 3 \times 3$); control and laser (Con-La, $n = 6 \times 3$); disuse (Dis, $n = 3 \times 3$); and disuse and laser (Dis-La, $n = 3 \times 3$). **b** HE staining of the TA muscle revealed that both Dis and Dis-La groups exhibited a smaller diameter of MFs than those in Con and Con-La groups as the muscular atrophy was observed in Dis and Dis-La groups since the 1st week of damage. Bar, 100 μm. **c** Consistent with the histological findings, a more well-preserved MF diameter was observed in the Dis-La group (32.05 ± 8.42 μm) than in the Dis group (24.95 ± 5.86 μm) at the 1st week ($p \leq 0.05$). However, this protective effect of LLL was observed for a limited period. Similar to the results of the Dis-La group, the MF diameter in the Con-La significantly increased compared to that in the Con group (59.2 ± 11.04 and 43.7 ± 3.19 μm, $p \leq 0.05$)

examination. A DS3 constant-current stimulator with a constant-current unit (CCU1; Upward Biosystems, Taipei, Taiwan) was used for performing EMG. The stimulation point and signal receiver (150 mm between the two points) were set at the upper and lower quarters of the muscle. The stimulation setting was 1 mA/20 ms, with a duration of 20 μs.

Toe lift test

A toe lift test was conducted to evaluate the maximum weight that the TA of the rats could lift up. A water bottle filled with baseline amount of water for weight bearing hanged by a plastic rope was tied up transversely to the middle of the right feet of a rat via a rubber band. Then, a pain stimulus was pressed on the middle phalanx of III digit of the right hind foot during each trial. A rat would have ankle dorsiflexion (TA muscle's response) after the pain stimuli. A total of 10 mL of water was, then, added to the water bottle iteratively. A 5-min break was taken between each consecutive 5 trials. The maximum volume that the test rats lifted in each group was recorded (Suppl. Fig. 3). The lifting motion is considered incomplete if the test foot did not touch the surface of the TA muscle. The test is judged as "Failure" when the rat failed to lift the bottle three times consecutively. Contrarily, the test is considered as "Pass" when the tested foot successfully touches the TA muscle. A break of 10 min was taken between every trial of lift up.

Statistical data

Data were presented as mean ± standard deviation (SD). Regarding the numerical parameters in Pax7 immunostaining, BrdU assay, and MTT assay, data were analyzed by one-way analysis of variance (ANOVA), and the post hoc tests were performed with Tukey's multiple-comparison test. As for the myofiber diameter, the data was analyzed by paired *t* test. Lastly, the numerical parameters in EMG, toe lift test, and Pax7-MyoD-Tunel population identification were analyzed via unpaired *t* test. Once the level of significance was equal to or less than 0.05 ($p \leq 0.05$), statistical difference was considered. Statistic data were processed by Microsoft Excel 2010 and GraphPad Prism 5.

Results

LLL irradiation for 7 s effectively enhanced the proliferation of Pax7^{+ve} cells isolated from TA muscle

The experiment to identify the optimal irradiation condition enhancing the proliferation of the Pax7^{+ve} cells, which were isolated from TA muscle, was performed. The condition of 0, 3, 7, 10, and 15 s was irradiated, respectively, and the irradiated cells were fixed and immunostained with the Pax7 antibody and BrdU assayed 48 h later (Fig. 1a). The results were summarized in Fig. 1b, which showed a bell-shaped distribution, revealing maximal and significant irradiation effect at 7 s (7″, 1.23 ± 0.05, $p \leq 0.05$, $n = 3$). By contrast, a prolonged irradiation time, such as 15 s, was associated with reduced proliferation relative to the control group of 0 s (0.93 ± 0.17). To further confirm cell viability, we further conducted the MTT assay in each group (Fig. 1c). Consistent with the results of the BrdU assay, cell viability was the highest at 7 s (7″, 1.22 ± 0.13, $p = 0.08$, $n = 3$). Overall, we conducted the subsequent experiments with an irradiation time of 7 s.

Fig. 3 LLL irradiation temporarily preserved the contractility of TA muscle in the Dis-La group while an effective strengthened contractility was observed in the Con-La group. To functionally evaluate the protective effect of LLL irradiation, the EMGs were performed with each group. **a**,**b** Consistent with the results of HE staining, a higher amplitude was observed in the Dis-La group than in the Dis group at week one (4.02 ± 1.25 and 2.60 ± 0.34 mV, $p \leq 0.05$). In addition, the amplitude increased more significantly in the Con-La group than in the Con group, revealing the capability of LLL to strengthen the contractility of TA muscle in healthy rat (Con-La, 9.03 ± 2.31 and 4.60 ± 0.60 mV, $p \leq 0.05$). **c** To precisely evaluate the muscle power of the LLL-irradiated TA muscle, the toe lift test was performed with each group. In concordance with the EMG results, contractility of TA muscle was transiently preserved in the Dis-La group (125 ± 5.77 g, day 9, $p \leq 0.05$, $n = 3$), and, simultaneously, an increased contractility of TA muscle in the Con-La group to 197.5 ± 9.57 g (day 21, $p \leq 0.05$) was observed, which is a 21% increase in the maximum weight compared with that in the Con group

LLL irradiation temporarily delays atrophy progression by preserving the muscle mass in the disuse-induced atrophy model

After confirming the optimal irradiation condition to promote the proliferation of Pax7^{+ve} cell within TA muscle, the analysis of LLL irradiation effect on disuse-induced atrophy model was examined. We classified the experimental animals into the following four groups: control (Con, $n = 3 \times 3$; 3 rats per experiment were used and each experiment was repeated 3 times); control with LLL irradiation (Con-La, $n = 6 \times 3$); disuse (Dis, $n = 3 \times 3$); and disuse with LLL irradiation (Dis-La, $n = 3 \times 3$). Each group was analyzed respectively at 1, 2, and 3 weeks after the damage (Fig. 2a). Figure 2b showed the results of HE staining of TA muscles in each group, and the average diameter of myofiber (MF) of each group was measured. Although both groups revealed remarkable atrophy, Dis-La group of 1 week showed a significant preservation of MF size compared to that in Dis group which received no LLL irradiation (32.05 ± 8.42 and 24.95 ± 8.42 μm, $p \leq$

a

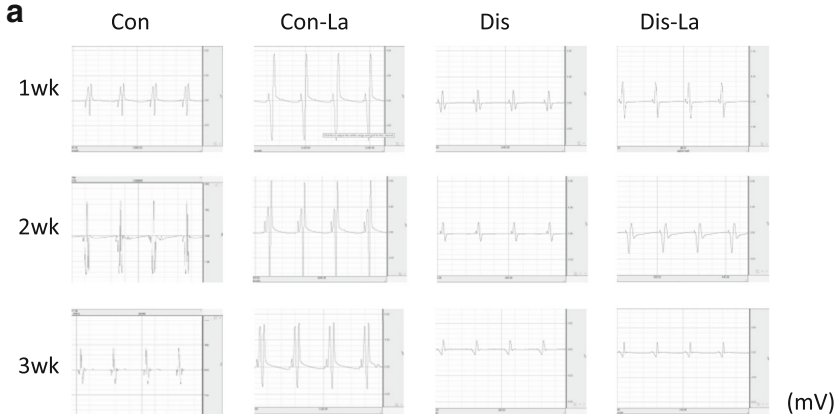

b

n=3	Con	Con-La	Dis	Dis-La
1wk	4.60±0.60	9.03±2.31**	2.60±0.34	4.02±1.25*
2wk	5.87±4.31	7.87±1.85**	2.53±0.12	2.70±0.70
3wk	4.93±2.20	8.20±1.98**	1.55±0.74	1.76±0.75

(mV)

Unpaired t-test, * $p \leq 0.05$ relative to Dis , ** $p \leq 0.05$ relative to Con

c

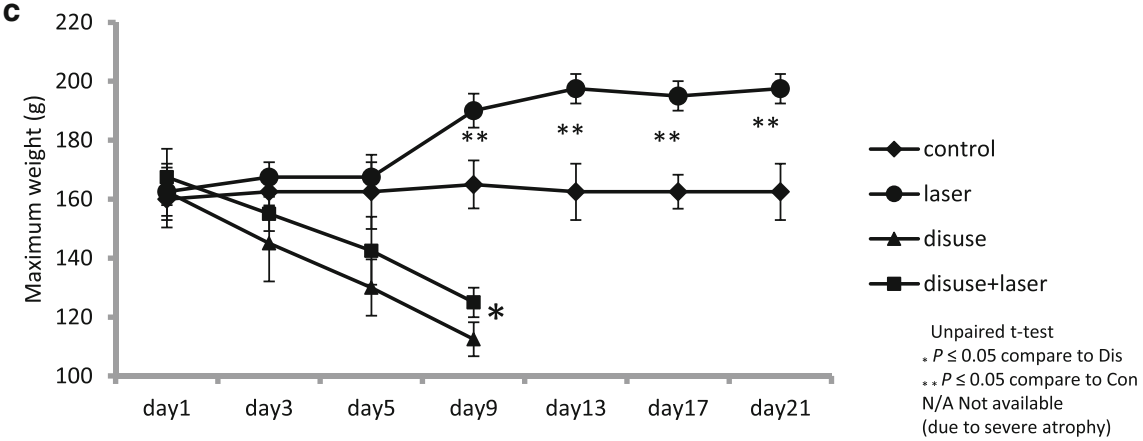

	Con	Con-La		Dis	Dis-La	
day1	160±8.16	162.5±9.57		162.5±9.57	167.5±9.57	
day3	162.5±5	167.5±5		145±5.77	155±12.91	
day5	162.5±5	167.5±12.58		130±11.55	142.5±9.57	
day9	165±5.77	190±8.16	**	112.5±5	125±5.77	*
day13	162.5±5	197.5±9.57		N/A	N/A	
day17	162.5±5	195±5.77		N/A	N/A	
day21	162.5±5	197.5±9.57		N/A	N/A	

(g)

0.05, Fig. 2b,c). However, this protective effect of LLL was observed for only a limited period of no longer than 2 weeks after the damage. Notably, the average MF diameter of TA muscle in the Con-La group increased significantly, relative to that in the Con group (59.2 ± 11.04 and 43.7 ± 3.19 μm, $p \leq 0.05$; Fig. 2b,c).

LLL irradiation temporarily preserved the contractility of TA muscle in Dis-La group while an effectively strengthened contractility was observed in Con-La group

In order to evaluate the contractility of TA muscle, the EMG (Fig. 3a,b) and the toe lift test (Fig. 3c) were arranged for each group. The contractility of TA muscle in the Dis-La group at 1 week was significantly preserved relative to that in the Dis group (4.02 ± 1.25 and 2.60 ± 0.34 mV, $p \leq 0.05$; Fig. 3a,b), though the contractility of TA muscle in the Dis-La had declined gradually in 2 and 3 weeks (2.70 ± 0.70 and 1.76 ± 0.75 mV; Fig. 3a,b). This protective effect of LLL was further confirmed by the toe lift test. In the test, the average maximum weight in which the Dis-La group lifted up was 125 ± 5.77 g, which was significantly higher than 112.5 ± 5 g of the Dis group (day 9, $p \leq 0.05$; Fig. 3c). On the other hand, consistent to the results of myofiber size, an enhanced muscle contractility (+ 15%) was observed in the Con-La group relative to that in the Con group from day 9 (190 ± 8.16 and 165 ± 5.77 g, $p \leq 0.05$; Fig. 3c).

The number of activated SCs expressing $Pax7^{+ve}MyoD^{+ve}$ was transiently increased and their ratio of apoptosis was suppressed simultaneously in Dis-La group

Although temporally, LLL demonstrated a protective effect in decelerating the progression of atrophy in disuse-induced atrophy model. Furthermore, LLL showed its capability to enhance the contractility of intact TA muscle (Con-La). Since both regeneration and hypertrophy of the skeletal muscle are well-recognized to closely rely on SC activation and its myogenic differentiation, the change in the number of activated SC, which expressed $Pax7^{+ve}MyoD^{+ve}$, was evaluated for each group sequentially from 1 to 3 weeks. Furthermore, in order to reveal the relationship between activated SC and cell apoptosis, TUNEL assays were performed concurrently with immunostaining of Pax7 and MyoD (Fig. 4a). The results clearly revealed that along with the significant increase in the number of activated SC ($Pax7^{+ve}MyoD^{+ve}$) in Dis-La (58.1 ± 5.1, $p \leq 0.05$; Fig. 4b, upper panel), the ratio of apoptotic activated SC ($Pax7^{+ve}MyoD^{+ve}Tunel^{+ve}$) was remarkably decreased in 1 week, relative to that in the Dis group (33.4 ± 0.05, $p \leq 0.05$; Fig. 4b, upper panel). However, these proliferative and protective effects of LLL to SC in disuse-induced atrophy were only observed temporarily, no longer than 1 week. In fact, the number of activated SC was remarkably reduced (32.8 ± 4.2 and 27.5 ± 4.5; Fig. 4b, upper panel) while the ratio of apoptotic activated SC was significantly increased in 2 and 3 weeks (54.9 ± 0.11 and 69.8 ± 0.07; Fig. 4b, upper panel). Compatible to the increase in apoptosis ratio in activated SC, the number of lineage-committed SC ($Pax7^{-ve}MyoD^{+ve}$) in both Dis and Dis-La was also declined (27.2 ± 4.4, 18.6 ± 2.4, 15.6 ± 2.5 and 28.7 ± 2.4, 19.2 ± 3.9, 12.1 ± 3.4; Fig. 4b, lower panel). Besides Dis and Dis-La groups, the changes of $Pax7^{+ve}MyoD^{+ve}$ and $Pax7^{-ve}MyoD^{+ve}$ cell numbers in Con and Con-La groups were also assessed. Resembling the results in Dis-La, Con-La showed a significant increase in $Pax7^{+ve}MyoD^{+ve}$ cell number but a decline in $Pax7^{+ve}MyoD^{+ve}Tunel^{+ve}$ cell number (Fig. 4c, upper panel). However, unlike transient effect in Dis-La, the number of $Pax7^{-ve}MyoD^{+ve}$ cell in Con-La remained significantly higher than that in Con until 3 weeks (46.2 ± 5.1, 50.12 ± 4.5, 43.77 ± 4.6 and 32.15 ± 6.4, 34.29 ± 5.7, 33.58 ± 4.3; Fig. 4c, lower panel).

Discussion

Although muscular atrophy has an intimate involvement in one's quality of life, rehabilitation remains as the only practicable clinical option to delay its progression currently. Nevertheless, rehabilitation has apparent limitation either to effectively stop the progression of atrophy or to improve the condition of atrophy. Considerable efforts have been dedicated to establishing novel treatments [36–38]; however, matured biological techniques and credible experimental data are still lacking for their clinical application. To find a novel treatment, most importantly possessing a potential for clinical application, we draw our attention onto LLL. LLL has already been applied clinically as a medical apparatus for pain control [39]; in addition, studies have proved its capability to enhance SC proliferation and inhibit their apoptosis in vitro [32–34]. Although the protective effect of LLL on denervation-induced atrophy was reported [31, 40], its competence for secondary atrophy, such as disuse-induced atrophy, remains unknown. Since SC plays a key role during postnatal muscle regeneration, a beneficial effect of LLL to disuse-induced atrophy is expected. In this study, we applied LLL irradiation on the TA muscle of disuse-induced atrophy model of rat and evaluated its effect by subjecting the muscle to morphological, histological, electrophysiological, and motor functional analyses. Particularly, the change in SC number was compared between the Dis and Dis-La groups. In the Dis group, corresponding the damage of disuse, SCs were quickly activated ($Pax7^{+ve}MyoD^{+ve}$) and rapidly proliferated, though, along the increase of activated SCs, the ratio of apoptosis within the population ($Pax7^{+ve}MyoD^{+ve}Tunel^{+ve}$/$Pax7^{+ve}MyoD^{+ve}$) was elevated simultaneously. As a consequence, both the number and the ratio of cell that reflected a successful differentiation and committed to myogenic lineage ($Pax7^{-ve}MyoD^{+ve}$ and $Pax7^{-ve}MyoD^{+ve}Tunel^{-ve}$/MF) were declined. In contrast, in the Dis-La group, LLL showed a capability to effectively enhance the proliferation of activated SC relative to that in Dis.

a

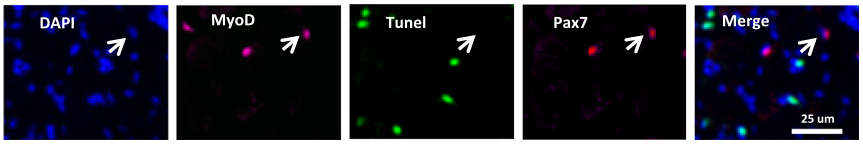

b

	Dis 1wk	Dis-La 1wk	Dis 2wk	Dis-La 2wk	Dis 3wk	Dis-La 3wk
$Pax7^{+}MyoD^{+}$ (A)	48.3±5.6	58.1±5.1*	34.2±3.5	32.8±4.2	28.1±2.1	27.5±4.5
$Pax7^{+}MyoD^{+}Tunel^{+}$ (B)	20.5±3.2	19.4±3.7	19.5±2.3	17.7±3.4	17.7±1.5	19.2±2.7
Apoptosis ration (B/A, %)	42.4±0.06	33.4±0.05*	57.0±0.14	54.9±0.11	63.0±0.12	69.8±0.07
$Pax7^{+}MyoD^{+}Tunel^{-}$/MF	0.061±0.002	0.085±0.003*	0.025±0.003	0.026±0.002	0.019±0.004	0.016±0.002
$Pax7^{-}MyoD^{+}$ (A)	27.2±4.4	28.7±2.4	18.6±2.4	19.2±3.9	15.6±2.5	12.1±3.4
$Pax7^{-}MyoD^{+}Tunel^{+}$ (B)	18.3±2.5	18.6±1.8	13.2±2.4	13.3±2.8	10.5±1.5	7.1±1.6
Apoptosis ratio (B/A, %)	67.28±0.05	64.81±0.06	70.97±0.04	69.27±0.07	67.31±0.10	58.68±0.06
$Pax7^{-}MyoD^{+}Tunel^{-}$ /MF	0.019±0.002	0.022±0.001*	0.009±0.001	0.010±0.001	0.009±0.001	0.010±0.000

MF: myofiber
Unpaired t-test, * relative to Dis , $p \leq 0.05$

c

	Con 1wk	Con-La 1wk	Con 2wk	Con-La 2wk	Con 3wk	Con-La 3wk
$Pax7^{+}MyoD^{+}$ (A)	28.6±3.5	30.5±3.1	28.4±3.5	33.2±2.4	30.5±3.1	26.7±2.8
$Pax7^{+}MyoD^{+}Tunel^{+}$ (B)	5.7±1.2	2.8±0.7*	5.9±1.9	2.5±0.4*	5.8±0.8	2.4±0.4*
Apoptosis ratio (B/A, %)	19.93±0.02	9.18±0.02*	20.77±0.09	7.53±0.01*	19.02±0.21	8.99±0.03*
$Pax7^{+}MyoD^{+}Tunel^{-}$/MF	0.067±0.004	0.077±0.005*	0.048±0.002	0.078±0.005*	0.046±0.003	0.069±0.003
$Pax7^{-}MyoD^{+}$ (A)	32.15±6.4	46.21±5.1*	34.29±5.7	50.12±4.5*	33.58±4.3	43.77±4.6*
$Pax7^{-}MyoD^{+}Tunel^{+}$ (B)	15.17±2.4	10.28±1.5*	16.48±3.1	14.84±2.6	17.61±2.6	11.15±3.4*
Apoptosis ratio (B/A, %)	47.19±0.02	22.25±0.03*	48.06±0.02	29.61±0.04*	52.44±0.03	24.47±0.04*
$Pax7^{-}MyoD^{+}Tunel^{-}$/MF	0.041±0.005	0.090±0.003*	0.041±0.002	0.082±0.004*	0.038±0.003	0.085±0.007*

MF: myofiber
Unpaired t-test, * relative to Con, $p \leq 0.05$

Fig. 4 The number of activated SCs expressing $Pax7^{+ve}MyoD^{+ve}$ was transiently increased, and their ratio of apoptosis was suppressed simultaneously in the Dis-La group. **a** To determine the effect of LLL on activated SCs, particularly on their apoptosis, the immunostaining of Pax7, MyoD, and TUNEL was performed (an activated SC which expressed as $Pax7^{+ve}MyoD^{+ve}Tunel^{-ve}$ was indicated by white arrow). **b** The number of activated SC ($Pax7^{+ve}MyoD^{+ve}$) increased (58.1 ± 5.1, $p \leq 0.05$) while a decreased apoptotic ratio (33.4 ± 0.05, $p \leq 0.05$) was observed in Dis-La, which suggested an enhanced proliferation and a protective effect against apoptosis of activated SC. **c** (upper panel) Resembling Dis-La, Con-La was observed to have promoted proliferation and a reduced apoptotic ratio of SC (30.5 ± 3.1 and 9.18 ± 0.02%, $p \leq 0.05$). **b**,**c** (lower panel) In contrast to the result of Dis-La, a significant elevation in the number of myogenic lineage-committed SC ($Pax7^{-ve}MyoD^{+ve}$, 46.21 ± 5.1, 50.12 ± 4.5and 43.77 ± 4.6, $p \leq 0.05$) was consistently observed in Con-La

Furthermore, LLL reduced the ratio of apoptosis in activated SC, thereby increasing the ratio of cell that had successfully committed to myogenic lineage ($Pax7^{-ve}MyoD^{+ve}Tunel^{-ve}$/MF) and, hence, preserved the contractility of the TA muscle. Unfortunately, this protective effect of LLL was only observed within one week, as the number of $Pax7^{-ve}MyoD^{+ve}$ (myogenic lineage committed) cell quickly dropped and the number of apoptotic $Pax7^{-ve}MyoD^{+ve}$ (myogenic lineage committed) cell rapidly elevated. As a consequence, there was no significant statistical difference observed between the Dis-La and Dis groups since the second week post-damage. These results revealed that although LLL was capable in enhancing the proliferation of SC ($Pax7^{+ve}MyoD^{+ve}$) during muscle regeneration induced by disuse, the proliferated SCs were not able to complete the process of differentiation, particularly to successfully commit to myogenic lineage ($Pax7^{-ve}MyoD^{+ve}$). As a result, these SCs with impaired capability in maturation become apoptotic ($Pax7^{+ve}MyoD^{+ve}Tunel^{+ve}$). Only transiently LLL showed its capability to delay the progression of apoptosis in the activated SC, thereby temporally postponing the progression of atrophy.

In addition to the disuse-induced atrophy model, LLL irradiation was applied onto the control group of healthy rat (Con-La). Interestingly, compatible to the increase in myofiber diameter, a stronger contractility was observed in the Con-La group relative to that in the control. Resembling the Dis-La group, which received LLL irradiation, Con-La was confirmed to also show a significant increase in the SC number but a remarkable decrease in its apoptosis ratio. Unlike Dis-La, the effect of LLL in Con-La had persisted until the third week. Therefore, in Con-La, the number of $Pax7^{-ve}MyoD^{+ve}$ (myogenic lineage committed) was continuously higher and the ratio of $Pax7^{-ve}MyoD^{+ve}Tunel^{-ve}$/MF (apoptotic myogenic lineage committed cell) was consistently lower than that in the Con group. One thing that should be noted was since the toe lift up test was a test comprised of daily movement of tested foot, the test itself could be considered as a regular contraction training. Taken together, these results suggested an indispensable role of muscle contraction during SC maturation, in particular, for the process of myogenic lineage commitment in SC, a process that is characterized by the down-regulation of Pax7 and up-regulation of MyoD expression. Otherwise, apoptosis could be occurred within those SCs which failed to complete the myogenic differentiation and lead to a state of muscular atrophy eventually. In contrary, when LLL irradiation was combined with regular muscle contraction, an enhanced muscle contractility was observed compared to the group that was performed with contraction alone, and this result was compatible with the result of Nakano et al. [35]. Since the combination of LLL irradiation and muscular contraction was only performed with healthy rat in this study, it is interesting how the combination of LLL and muscular contraction act on the disuse-induced atrophy model.

In conclusion, though transiently, this is the first study to demonstrate the capability of LLL in delaying the speed of disuse-induced atrophy through the enhancement of activated SC ($Pax7^{+ve}MyoD^{+ve}$) proliferation while protecting them from apoptosis at the same time. However, this effect of LLL was observed within a limited period of one week, thus temporarily preserving its motor function. In addition, this study also confirmed muscle contraction as an indispensable factor for successful muscle maturation, particularly for the step of myogenic commitment of SC. Last, but not the least, contractility was strengthened when LLL was applied onto normal healthy rats with a combination of muscle contraction, suggesting a novel potential clinical application of LLL in prevention of muscular atrophy.

Acknowledgments We thank our colleague, Yu-Shan Lin, who has contributed to the concepts and experiments in this manuscript.

Funding This study was supported by the Grant-in-Aid for Scientific Research TMU100-AE1-B10, 101TMU-TMUH-11 from the Taipei Medical University, and the Taipei Medical University Hospital and Grant-in-Aid for Scientific Research 101-2314-B-038-017-MY3 from the Ministry of Science and Technology, R.O.C., Taiwan.

Compliance with ethical standards

Conflict of interests The authors declare that they have no competing or financial interests. The authors also certify that they have no affiliations with or involvement in any organization or entity with any financial interest or non-financial interest in the subject matter or materials discussed in this manuscript.

References

1. Brook MS, Wilkinson DJ, Phillips BE, Perez-Schindler J, Philp A, Smith K, Atherton PJ (2016) Skeletal muscle homeostasis and plasticity in youth and ageing: impact of nutrition and exercise. Acta Physiol (Oxf) 216(1):15–41. https://doi.org/10.1111/apha.12532
2. Janssen I, Heymsfield SB, Wang ZM, Ross R (2000) Skeletal muscle mass and distribution in 468 men and women aged 18-88 yr. J Appl Physiol (Bethesda, MD: 1985) 89(1):81–88. https://doi.org/10.1152/jappl.2000.89.1.81
3. Ferrans CE, Lipscomb J, Gotay CC, Snyder C (2004) Outcome assessment in cancer, definitions and conceptual models of quality of life. Cambridge University Press
4. Cezar CA, Mooney DJ (2015) Biomaterial-based delivery for skeletal muscle repair. Adv Drug Deliv Rev 84:188–197. https://doi.org/10.1016/j.addr.2014.09.008
5. Mauro A (1961) Satellite cell of skeletal muscle fibers. J Biophys Biochem Cytol 9:493–495
6. Seale P, Sabourin LA, Girgis-Gabardo A, Mansouri A, Gruss P, Rudnicki MA (2000) Pax7 is required for the specification of myogenic satellite cells. Cell 102(6):777–786
7. Rudnicki MA, Schnegelsberg PN, Stead RH, Braun T, Arnold HH, Jaenisch R (1993) MyoD or Myf-5 is required for the formation of skeletal muscle. Cell 75(7):1351–1359
8. Kuang S, Kuroda K, Le Grand F, Rudnicki MA (2007) Asymmetric self-renewal and commitment of satellite stem cells in muscle. Cell 129(5):999–1010. https://doi.org/10.1016/j.cell.2007.03.044
9. Rudnicki MA, Le Grand F, McKinnell I, Kuang S (2008) The molecular regulation of muscle stem cell function. Cold Spring Harb Symp Quant Biol 73:323–331. https://doi.org/10.1101/sqb.2008.73.064
10. McCullagh KJ, Perlingeiro RC (2015) Coaxing stem cells for skeletal muscle repair. Adv Drug Deliv Rev 84:198–207. https://doi.org/10.1016/j.addr.2014.07.007
11. Seale P, Rudnicki MA (2000) A new look at the origin, function, and "stem-cell" status of muscle satellite cells. Dev Biol 218(2):115–124. https://doi.org/10.1006/dbio.1999.9565
12. Zammit PS, Heslop L, Hudon V, Rosenblatt JD, Tajbakhsh S, Buckingham ME, Beauchamp JR, Partridge TA (2002) Kinetics of myoblast proliferation show that resident satellite cells are competent to fully regenerate skeletal muscle fibers. Exp Cell Res 281(1):39–49
13. Benedini-Elias PC, Morgan MC, Gomes AR, Mattiello-Sverzut AC (2009) Changes in postnatal skeletal muscle development induced by alternative immobilization model in female rat. Anat Sci Int 84(3):218–225. https://doi.org/10.1007/s12565-009-0016-3
14. Marimuthu K, Murton AJ, Greenhaff PL (2011) Mechanisms regulating muscle mass during disuse atrophy and rehabilitation in humans. J Appl Physiol (Bethesda, MD: 1985) 110(2):555–560. https://doi.org/10.1152/japplphysiol.00962.2010
15. Lecker SH, Jagoe RT, Gilbert A, Gomes M, Baracos V, Bailey J, Price SR, Mitch WE, Goldberg AL (2004) Multiple types of skeletal muscle atrophy involve a common program of changes in gene

expression. FASEB J 18(1):39–51. https://doi.org/10.1096/fj.03-0610com
16. Nawrotzki R, Blake DJ, Davies KE (1996) The genetic basis of neuromuscular disorders. Trends Genet 12(8):294–298
17. Deitrick JE (1948) The effect of immobilization on metabolic and physiological functions of normal men. Bull N Y Acad Med 24(6): 364–375
18. Tomanek RJ, Lund DD (1973) Degeneration of different types of skeletal muscle fibres. I Denervation. J Anat 116(Pt 3):395–407
19. Zeman RJ, Zhao J, Zhang Y, Zhao W, Wen X, Wu Y, Pan J, Bauman WA, Cardozo C (2009) Differential skeletal muscle gene expression after upper or lower motor neuron transection. Pflugers Archiv Eur J Physiol 458(3):525–535. https://doi.org/10.1007/s00424-009-0643-5
20. Bruusgaard JC, Gundersen K (2008) In vivo time-lapse microscopy reveals no loss of murine myonuclei during weeks of muscle atrophy. J Clin Invest 118(4):1450–1457. https://doi.org/10.1172/jci34022
21. Wan Q, Yeung SS, Cheung KK, Au SW, Lam WW, Li YH, Dai ZQ, Yeung EW (2016) Optimizing electrical stimulation for promoting satellite cell proliferation in muscle disuse atrophy. Am J Physical Med Rehabil 95(1):28–38. https://doi.org/10.1097/phm.0000000000000307
22. Passarella S, Casamassima E, Molinari S, Pastore D, Quagliariello E, Catalano IM, Cingolani A (1984) Increase of proton electrochemical potential and ATP synthesis in rat liver mitochondria irradiated in vitro by helium-neon laser. FEBS Lett 175(1):95–99
23. Alves AN, Fernandes KP, Melo CA, Yamaguchi RY, Franca CM, Teixeira DF, Bussadori SK, Nunes FD, Mesquita-Ferrari RA (2014) Modulating effect of low level-laser therapy on fibrosis in the repair process of the tibialis anterior muscle in rats. Lasers Med Sci 29(2): 813–821. https://doi.org/10.1007/s10103-013-1428-9
24. Iyomasa DM, Garavelo I, Iyomasa MM, Watanabe IS, Issa JP (2009) Ultrastructural analysis of the low level laser therapy effects on the lesioned anterior tibial muscle in the gerbil. Micron 40(4): 413–418. https://doi.org/10.1016/j.micron.2009.02.002
25. Conlan MJ, Rapley JW, Cobb CM (1996) Biostimulation of wound healing by low-energy laser irradiation. A review. J Clin Periodontol 23(5):492–496
26. Yaakobi T, Maltz L, Oron U (1996) Promotion of bone repair in the cortical bone of the tibia in rats by low energy laser (He-Ne) irradiation. Calcif Tissue Int 59(4):297–300
27. Rochkind S, Geuna S, Shainberg A (2009) Chapter 25: phototherapy in peripheral nerve injury: effects on muscle preservation and nerve regeneration. Int Rev Neurobiol 87:445–464. https://doi.org/10.1016/s0074-7742(09)87025-6
28. Bibikova A, Belkin V, Oron U (1994) Enhancement of angiogenesis in regenerating gastrocnemius muscle of the toad (Bufo viridis) by low-energy laser irradiation. Anat Embryol 190(6):597–602
29. Amaral AC, Parizotto NA, Salvini TF (2001) Dose-dependency of low-energy HeNe laser effect in regeneration of skeletal muscle in mice. Lasers Med Sci 16(1):44–51
30. Wollman Y, Rochkind S (1993) Muscle fiber formation in vitro is delayed by low power laser irradiation. J Photochem Photobiol B 17(3):287–290
31. Rochkind S, Shainberg A (2013) Protective effect of laser phototherapy on acetylcholine receptors and creatine kinase activity in denervated muscle. Photomed Laser Surg 31(10):499–504. https://doi.org/10.1089/pho.2013.3537
32. Ben-Dov N, Shefer G, Irintchev A, Wernig A, Oron U, Halevy O (1999) Low-energy laser irradiation affects satellite cell proliferation and differentiation in vitro. Biochim Biophys Acta 1448(3): 372–380
33. Shefer G, Oron U, Irintchev A, Wernig A, Halevy O (2001) Skeletal muscle cell activation by low-energy laser irradiation: a role for the MAPK/ERK pathway. J Cell Physiol 187(1):73–80. https://doi.org/10.1002/1097-4652(2001)9999:9999<::aid-jcp1053>3.0.co;2-9
34. Shefer G, Partridge TA, Heslop L, Gross JG, Oron U, Halevy O (2002) Low-energy laser irradiation promotes the survival and cell cycle entry of skeletal muscle satellite cells. J Cell Sci 115(Pt 7): 1461–1469
35. Nakano J, Kataoka H, Sakamoto J, Origuchi T, Okita M, Yoshimura T (2009) Low-level laser irradiation promotes the recovery of atrophied gastrocnemius skeletal muscle in rats. Exp Physiol 94(9):1005–1015. https://doi.org/10.1113/expphysiol.2009.047738
36. Chang H, Yoshimoto M, Umeda K, Iwasa T, Mizuno Y, Fukada S, Yamamoto H, Motohashi N, Miyagoe-Suzuki Y, Takeda S, Heike T, Nakahata T (2009) Generation of transplantable, functional satellite-like cells from mouse embryonic stem cells. FASEB J 23(6):1907–1919. https://doi.org/10.1096/fj.08-123661
37. Ramos J, Chamberlain JS (2015) Gene therapy for Duchenne muscular dystrophy. Expert Opin Orphan Drugs 3(11):1255–1266. https://doi.org/10.1517/21678707.2015.1088780
38. Mizuno Y, Chang H, Umeda K, Niwa A, Iwasa T, Awaya T, Fukada S, Yamamoto H, Yamanaka S, Nakahata T, Heike T (2010) Generation of skeletal muscle stem/progenitor cells from murine induced pluripotent stem cells. FASEB J 24(7):2245–2253. https://doi.org/10.1096/fj.09-137174
39. Nobrega C, da Silva EM, de Macedo CR (2013) Low-level laser therapy for treatment of pain associated with orthodontic elastomeric separator placement: a placebo-controlled randomized double-blind clinical trial. Photomed Laser Surg 31(1):10–16. https://doi.org/10.1089/pho.2012.3338
40. Rochkind S, Shainberg A (2017) Muscle response to complete peripheral nerve injury: changes of acetylcholine receptor and creatine kinase activity over time. J Reconstr Microsurg 33(5):352–357. https://doi.org/10.1055/s-0037-1598619